Final Project. DC Motor Speed Controller

Date : 2018. 12. 14
Team : 7
Student ID : 21500401
21600372
Name : Eom Hyun Sang
Song Yoon Kyoung

1. Purpose

The purpose of the final project is for the PID controller to control the angular velocity of the DC motor. Use an analog circuit to drive the DC motor and look at its characteristics. In addition, you can also use MATLAB to predict the transfer function of the motor. The PID controller is designed using an amplifier. Through MATLAB, we predict the response characteristics of the system in the time domain and the frequency domain based on the controller and examines the results through experiments. In this project, you will learn controller design through classic control theory.

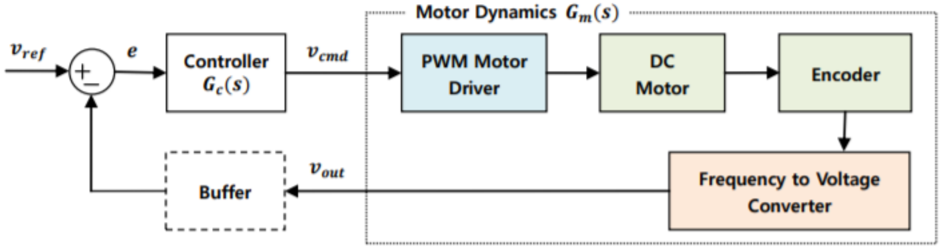

Figure 1. Closed-loop motor speed control system

2. Preliminary

2.1. Mathematical model of a DC motor with/without load

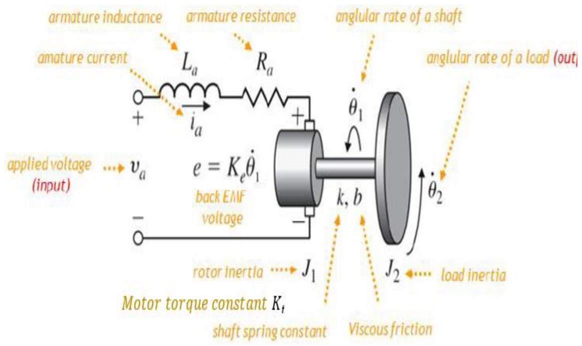

(a) Diagram with load

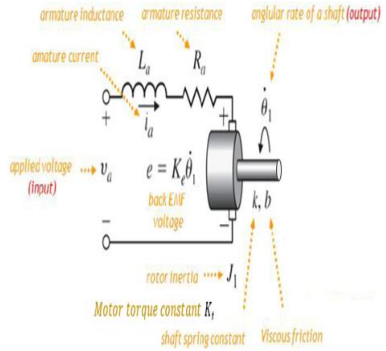

(b) Diagram without load

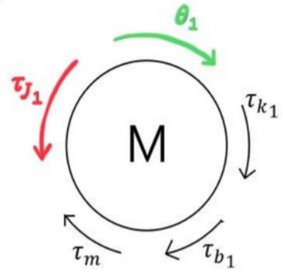

τ_m: motor torque
τ_{J1}: inertia torque
τ_{b1}: friction torque
τ_{k1}: spring torque

$$\tau_{J1} = J_1 \frac{d^2}{dt^2}\theta_1 \qquad \tau_{b1} = -b_m \frac{d}{dt}\theta_1$$

$$\tau_m = K_t i(t) \qquad \tau_{k1} = k(\theta_2 - \theta_1)$$

(b) Motor body

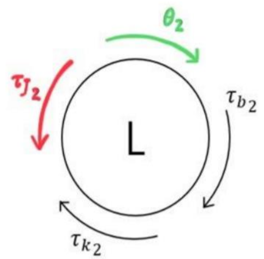

τ_{J2}: inertia torque
τ_{b2}: friction torque
τ_{k2}: spring torque

$$\tau_{J2} = J_2 \frac{d^2}{dt^2}\theta_2 \quad \tau_{b2} = b(\frac{d}{dt}\theta_1 - \frac{d}{dt}\theta_2)$$

$$\tau_{k2} = k(\theta_1 - \theta_2)$$

(c) Load

Figure 2. Permanent Magnet (PM) DC Motor

1) DC motor with load when the shaft is flexible ($\boldsymbol{k} \neq \infty \rightarrow \dot{\boldsymbol{\theta}}_1 \neq \dot{\boldsymbol{\theta}}_2$)

Motor is a system that converts electrical energy into physical energy. Therefore, it can be divided into electrical domain and mechanical domain.

· Electrical domain

First, R_a from the electrical domain in Figure (a) represents the motor resistance, and L_a is the coil inductance of the motor. When the rotating body of the motor rotates in the magnetic field, electromotive force is generated by Lenz's law. Therefore, applying the KVL rule that the sum of the voltage consumed by the motor and the supplied voltage is 0, the following differential equation can be obtained.

$$-v_a + L_a\frac{di_a}{dt} + R_a i_a + K_e\dot{\theta}_1 = 0 \tag{1}$$

By Laplace Transform

$$v_a(s) = (sL_a + R_a)I_a(s) + sK_e\theta_1(s) \tag{2}$$

· Mechanical domain

In terms of the mechanical domain, the motor torque generated by rotating the rotor of the motor is transmitted to the load through the shaft.

Motor body mechanical equation

$$K_t i_a = \mathrm{J}_1\ddot{\theta}_1 + b_m\dot{\theta}_1 + k(\theta_1 - \theta_2) \tag{3}$$

By Laplace Transform

$$K_t I_a(s) = s^2\mathrm{J}_1\theta_1(s) + sb_m\theta_1(s) + k(\theta_1(s) - \theta_2(s)) \tag{4}$$

Load mechanical equation

$$\mathrm{J}_2\ddot{\theta}_2 = b(\dot{\theta}_1 - \dot{\theta}_2) + k(\theta_1 - \theta_2) \tag{5}$$

By Laplace Transform

$$s^2\mathrm{J}_2\theta_2(s) = sb(\theta_1(s) - \theta_2(s)) + k(\theta_1(s) - \theta_2(s)) \tag{6}$$

· Block Diagram

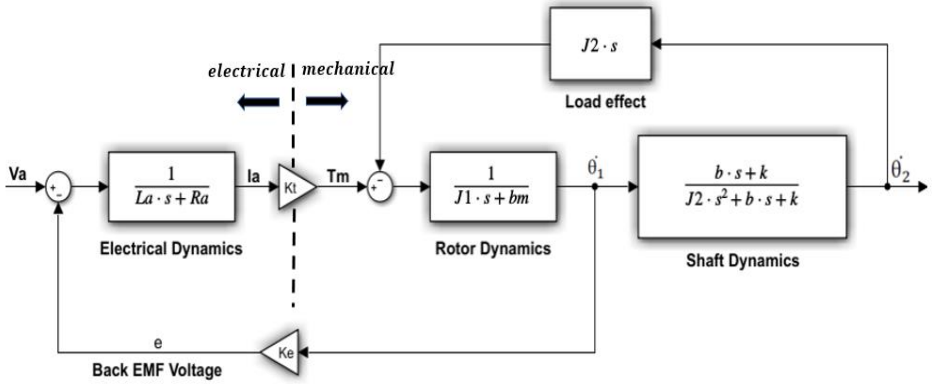

Figure 3. Block Diagram with load when the shaft is flexible

· Transfer function

$$\begin{aligned} \mathrm{G}(s) &= \frac{\dot{\theta}_2(s)}{V_a(s)}\left[\frac{\mathrm{rad}}{\mathrm{s}} * \frac{1}{\mathrm{V}}\right] \\ &= \frac{(bs+k)\,k_t}{(sL_a+R_a)\big((J_1 s + b_m)(J_2 s^2 + bs + k) + J_2 s(bs+k)\big) + K_e K_t(bs+k)} \end{aligned} \tag{7}$$

The motor transfer function is modeled in the form of 0 / 4 order form.

2) DC motor with load when the shaft is rigid ($k = \infty \rightarrow \dot{\theta}_1 = \dot{\theta}_2$)

When $k = \infty$, there is no axial friction coefficient and spring constant, so the angular displacement of the motor is equal to the angular displacement of the load. Simplifying the block diagram when the shaft is flexible results in a rigid shaft.

· **Block Diagram**

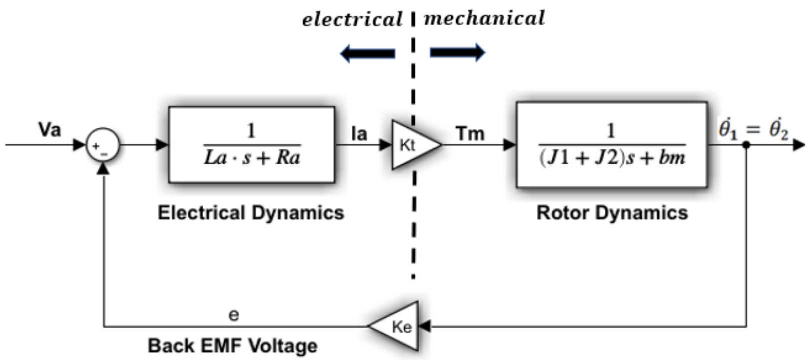

Figure 4. Block Diagram with load when the shaft is rigid

· **Transfer function**

$$\mathrm{G(s)} = \frac{\dot{\theta}_2(s)}{V_a(s)}\left[\frac{\mathrm{rad}}{\mathrm{s}} * \frac{1}{\mathrm{V}}\right]$$
$$= \frac{k_t}{(J_1+J_2)L_a s^2 + \left((J_1+J_2)R_a + L_a b_m\right)s + K_e K_t + R_a b_m} \quad (8)$$

The model transfer function is modeled as a 0 / 2 order form.

3) DC motor with load when electrical dynamics is negligible

Consider a pole of electrical dynamics and rotor dynamics when DC motor with load when the shaft is rigid. When Electrical dynamics is fast, the pole of Electrical dynamics is electrical dynamics is much faster than mechanical.

$$\left|-\frac{R_a}{L_a}\right| \cong \infty \gg \left|-\frac{b_m}{(J_1+J_2)}\right|$$

In this case, $L_a \rightarrow 0$.

· **Block Diagram**

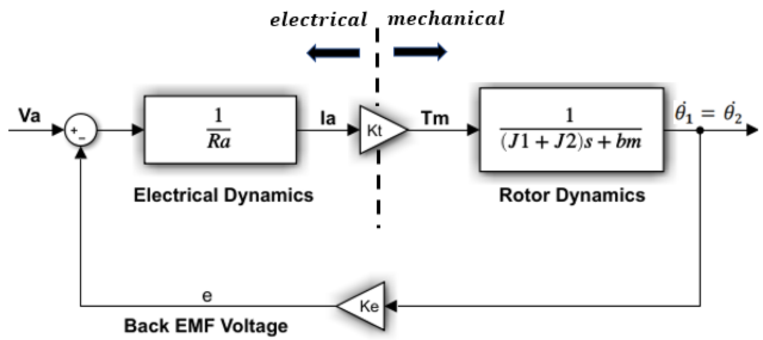

Figure 5. With load when electrical dynamics is negligible

· **Transfer function**

$$\mathrm{G(s)} = \frac{\dot{\theta}_2(s)}{V_a(s)}\left[\frac{\mathrm{rad}}{\mathrm{s}} * \frac{1}{\mathrm{V}}\right] = \frac{k_t}{(J_1+J_2)R_a s + (K_e K_t + R_a b_m)} \quad (9)$$

The model transfer function is modeled as a 0 / 1 order form.

4) DC motor without load

In the case of $J_2 = 0$, which is the load part, it can be considered as simplified.

· **Block Diagram**

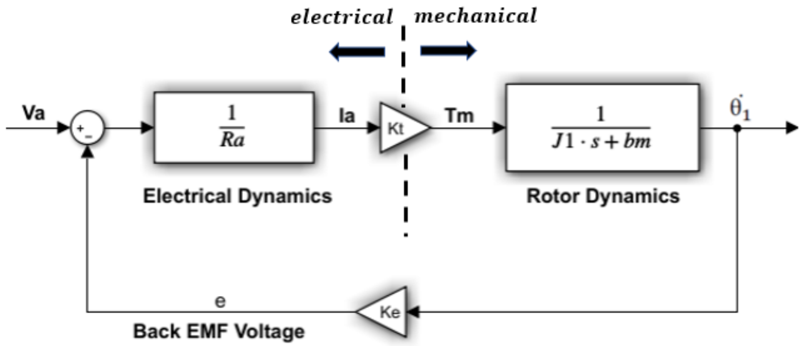

Figure 6. Block Diagram without load

· **Transfer function**

$$\begin{aligned} \mathrm{G(s)} &= \frac{\dot{\theta}_1(s)}{V_a(s)}\left[\frac{\mathrm{rad}}{\mathrm{s}} * \frac{1}{\mathrm{V}}\right] \\ &= \frac{k_t}{J_1 L_a s^2 + (J_1 R_a + L_a b_m)s + K_e K_t + R_a b_m} \end{aligned} \tag{10}$$

The model transfer function is modeled as a 0 / 2 order form.

Since the motor used in the experiment is a DC motor without load, look at the characteristic equation of a motor

$$s^2 + 2\zeta_m w_m s + w_m^2 = s^2 + \left(\frac{R_a}{L_a K_t} + \frac{b_m}{J_1 K_t}\right)s + \left(\frac{K_e}{J_1 L_a} + \frac{R_a b_m}{J_1 L_a K_t}\right) \tag{11}$$

The damping ratio (ζ_m) and the natural frequency (w_m) of the motor are affected by inertia or friction coefficients. It can be confirmed that the modeling of the motor varies depending on the difference in inertia or friction coefficient even for the same type of motor.

2.2. Time response of a second-order system

The response of a second-order system is characterized by two parameters, the natural frequency($\omega_n[rad/s]$), and the damping ratio($\zeta[-]$). Considering the characteristic equation

$$\Delta(s) = s^2 + 2\zeta\omega_n s + \omega_n^2 = 0 \quad \rightarrow \quad s_{1,2} = (-\zeta \pm j\sqrt{1-\zeta^2})\omega_n \tag{12}$$

When we see time response of under-damped system ($0 < \zeta < 1$)

$$\begin{aligned} c(t) = &\left(1 - \frac{1}{\sqrt{1-\zeta^2}} e^{-\zeta\omega_n t}\right. \\ &\left. \times \cos\left(\omega_n t\sqrt{1-\zeta^2} - \tan^{-1}\frac{\zeta}{\sqrt{1-\zeta^2}}\right)\right) u(t) \end{aligned} \tag{13}$$

1) Rise time ($t_r^{90}[\mathrm{s}]$)

: the time required for the step response to rise from 0% to 90% of its final value.

$$\begin{aligned} 0.9 = &\left(1 - \frac{1}{\sqrt{1-\zeta^2}} e^{-\zeta\omega_n t_r^{90}}\right. \\ &\left. \times \cos\left(\omega_n t_r^{90}\sqrt{1-\zeta^2} - \tan^{-1}\frac{\zeta}{\sqrt{1-\zeta^2}}\right)\right) u(t) \end{aligned} \tag{14}$$

2) Peak time ($T_p[\mathrm{s}]$)

: simply the time required by response to reach its first peak.

$$T_p = \frac{\pi}{\omega_n\sqrt{1-\zeta^2}}[\mathrm{s}] \tag{15}$$

3) %Over shoot ($\%OS$)

: . As the first peak of response is normally maximum in magnitude, maximum overshoot is simply normalized difference between first peak and steady-state value of a response.

$$\%OS = e^{-\left(\frac{\zeta}{\sqrt{1-\zeta^2}}\right)\pi} \times 100\% \tag{16}$$

4) Settling time ($T_s[s]$)

: the time required for the step response to stay within 2% of its final value. It is also observed that this duration is approximately 4 times of time constant of a signal.

$$T_s = \frac{4}{\zeta\omega_n}[s] \tag{17}$$

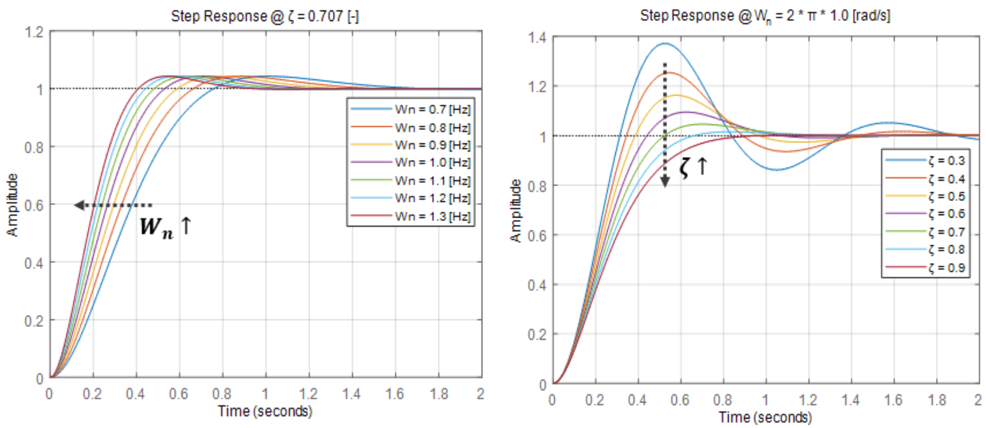

(a) $\zeta = 0.707[-]$ (b) $\omega_n = 2 * \pi * 1.0[rad/s]$

Figure 7. Step responses of a second-order system

According to figure 7(a), when ω_n increases, t_r^{90}decreases and speed of system increase.

According to figure 7(b), when ζ increases, $\%OS$ decreases.

2.3. Frequency response of a second-order system

Frequency response is the steady-state response of linear system when sinusoidal input signal that has frequency component. When the transfer function of the second system is $G(s)$, the frequency response can be expressed in terms of magnitude and phase.

$$G(s) = k * \frac{\omega_n^2}{s^2 + 2\zeta\omega_n s + \omega_n^2} \rightarrow G(j\omega) = \frac{k}{1 - \left(\frac{w}{\omega_n}\right)^2 + j2\zeta\left(\frac{w}{\omega_n}\right)} \tag{18}$$

When we see the magnitude

$$\begin{aligned} 20log|G(j\omega)| &= 20log\left|\frac{k}{1 - \left(\frac{\omega}{\omega_n}\right)^2 + j2\zeta\left(\frac{\omega}{\omega_n}\right)}\right| \\ &= -20log\left|1 - \left(\frac{\omega}{\omega_n}\right)^2 + j2\zeta\left(\frac{\omega}{\omega_n}\right)\right| \end{aligned} \tag{19}$$

When we see the phase

$$\angle G(j\omega) = \angle k - \angle\left(1 - \left(\frac{\omega}{\omega_n}\right)^2 + j2\zeta\left(\frac{\omega}{\omega_n}\right)\right) = -\tan^{-1}\left(\frac{2\zeta\left(\frac{\omega}{\omega_n}\right)}{1 - \left(\frac{\omega}{\omega_n}\right)^2}\right) \tag{20}$$

Table 1. Gain and phase according to frequency

	$\omega \ll \omega_n\ [rad/s]$	$\omega = \omega_n\ [rad/s]$	$\omega \gg \omega_n\ [rad/s]$
Gain[dB]	$20 * logk$	$20 * log\left\lvert\frac{k}{j2\zeta}\right\rvert$	$40 * log\omega$
Phase[deg]	0°	-90°	-180°

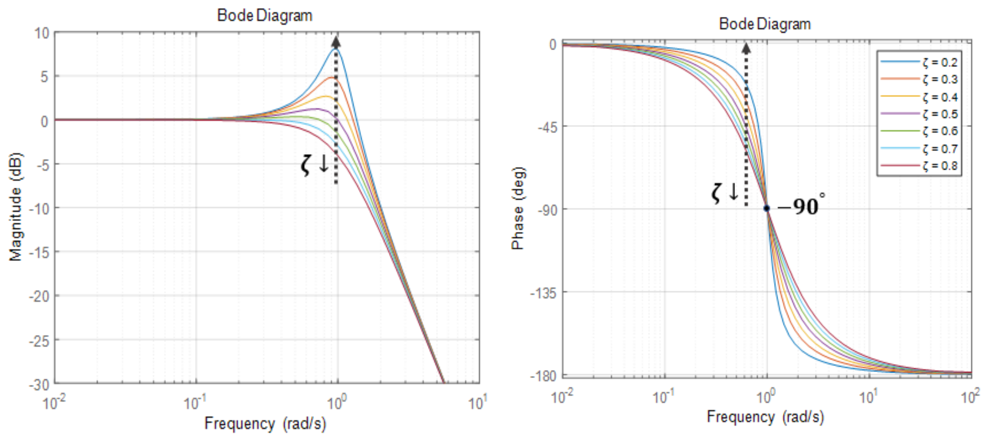

(a) Magnitude[dB] **(b) Phase[deg]**

Figure 8. Frequency responses of a second-order system

According to figure 8(a), Smaller damping result in larger resonance peck.

According to figure 8(b), Smaller damping yields smaller phase shift.

And phase shift at critical frequency is always -90[deg] regardless of damping ratio.

2.4. Steady-state error and System type

When the input is $R(s)$, steady-state error is difference between the input and output of a control system as $t \to \infty$.

$$e_{ss} = \lim_{s\to 0} sE(s) = \lim_{s\to 0} \frac{sR(s)}{1 + G_o(s)} \tag{23}$$

Factors affecting e_{ss} include system type, input / output type, and system parameter uncertainty.

The system type is defined by the number of pure integrators in the open-loop transfer function ($G_o(s)$). The system type plays an important role in determining the controller structure.

Table 2. System type and tracking performance

	Type 0		**Type 1**		**Type 2**	
Input	**Static error constant**	**Error**	**Static error constant**	**Error**	**Static error constant**	**Error**
Step $= Ku(t)$	$K_p = \text{Const}$	$\frac{K}{1+G(0)}$	$K_p = \infty$	0	$K_p = \infty$	0
Ramp $= Ktu(t)$	K_v	∞	$K_v = \text{Const}$	$\lim_{s\to 0}\frac{K}{sG(s)}$	$K_v = \infty$	0
Parabola $= \frac{K}{2}t^2u(t)$	K_a	∞	K_a	∞	$K_a = \text{Const}$	$\lim_{s\to 0}\frac{K}{s^2G(s)}$

3. Motor Dynamics Modeling

3.1. $v_{cmd}[\mathrm{V}] - v_{out}[\mathrm{V}]$ modeling

Theoretically, control is done in a liner system However, in fact, many of the plants we want to control are non-liner systems. The DC motors we use in our experiments also have non-liner properties. Therefore, one point of the $v_{cmd} - v_{out}$ characteristic curve of the DC motor is set as the operating point, and the system is controlled on the assumption that the part is liner.

Figure1 is the $v_{cmd} - v_{out}$ characteristic curve of the DC motor that shows the DC voltage applied to the DC motor at 0.1[V] intervals. Fingure1 shows that the DC motor has non-liner characteristics. In addition, the DC motor is divided into dead zone, liner region, and saturation region. The dead point of the motor is 1.4[V] and the saturation point is 3.2[V]. Therefore, it is assumed that liner is set by setting the 2[V] point of the liner region of this motor.

Since the motor is used in a linear region, it can be assumed to be an LTI system.

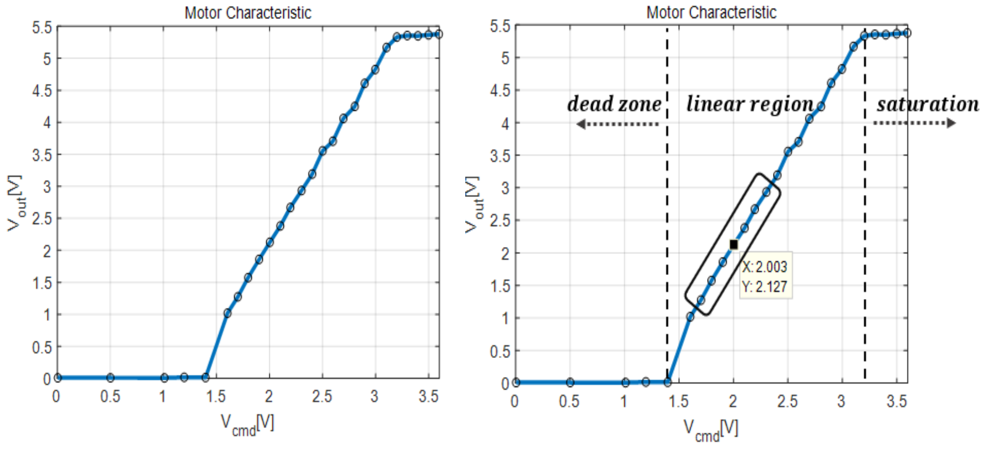

(a) Data Plot **(b) Operating Region**

Figure 9. $v_{cmd}[\mathrm{V}] - v_{out}[\mathrm{V}]$ **Characteristic Curve**

3.2. Frequency response

In the function generator, a sin wave with a DC offset of 2[V] (operating point) and a magnitude of 0.3[V] was put in to find the order of the DC motor and the expected control width. It is possible to check the order of the DC motor through the phase delay. The phase delay occurs 90 degrees in each pole. So, 90 degrees in the first-order system and 180 [deg] in the second-order system. The motor we use has a phase delay greater than 90 [deg], so we can see that the motor is a second-order system.

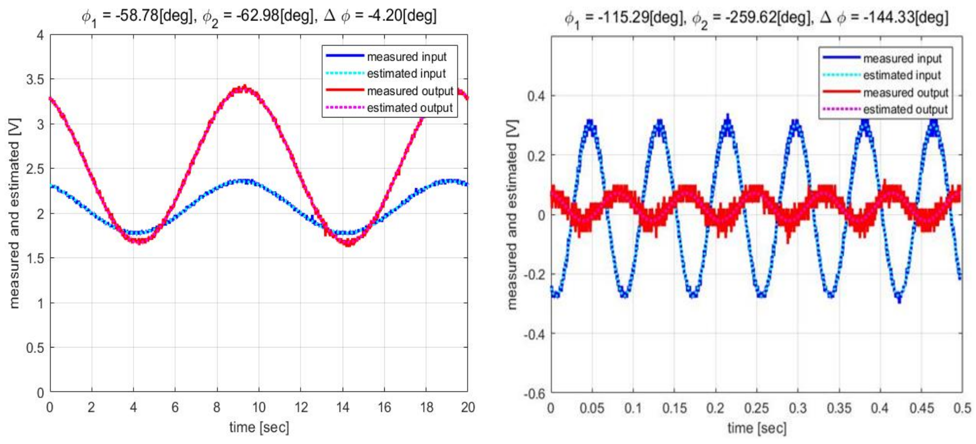

(a) When $f_{in} = \mathbf{0.1[Hz]}$ **(b) When** $f_{in} = \mathbf{12.0[Hz]}$

Figure 10. $v_{in}[\mathrm{V}] - v_{out}[\mathrm{V}]$ **of DC Motor**

The graph above shows the motor output when the frequency is $0.1[\mathrm{Hz}]$and $12.0[\mathrm{Hz}]$, respectively. From this data, as the frequency becomes smaller, the phase delay becomes closer to 0 and as the frequency becomes larger, the phase delay increases.

Since the motor is a second-order system, the predictable control width of this motor is about 90 degrees. Therefore, by adjusting the frequency, the point at 90 degrees becomes ω_c. As a result, it was confirm that the phase difference was 90 degrees at $3.8[\mathrm{Hz}]$and therefore, $\omega_c = 3.8 * 2\pi[\mathrm{rad/s}]$ was set.

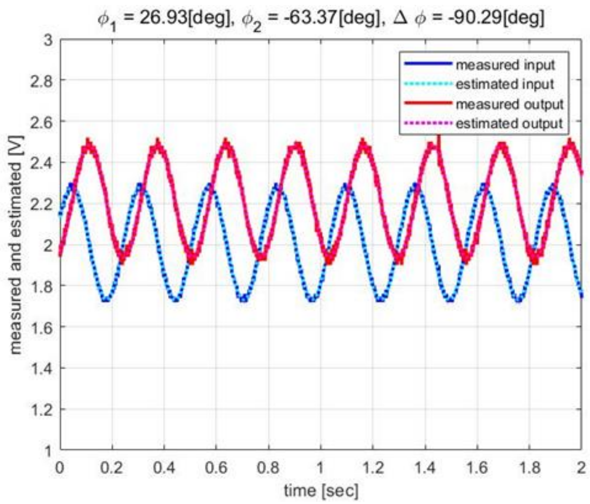

Figure 11. Check the system and Find the $f_c = 3.8[\mathrm{Hz}]$

3.3. Open loop transfer function of the DC motor including tachometer

The frequency sweep method was used at low frequencies because the uncertainty increases with increasing frequency.

Based on the predictable control width ($\omega_c[rad/s]$), the transfer function can be predicted by grabbing several points between

$$\frac{1}{10}f_c \le f_i \le \frac{1}{3}f_c \xrightarrow{\omega_i=2\pi f_i} \frac{1}{10}\omega_c \le \omega_i \le \frac{1}{3}\omega_c$$

Let us find the range of ω_i based on $\omega_c = 3.8 * 2\pi[\mathrm{rad/s}]$.

$$0.38 * 2\pi[\mathrm{rad/s}] \le \omega_i \le 1.27 * 2\pi[\mathrm{rad/s}]$$

The results obtained by holding 10 points within the range of ω_i for the DC motor are shown in the following Table 1.

Table 3. Setting Point of ω_i

ω_i [rad/s]	0.3	0.4	0.5	0.6	0.7
$\lvert G_m(j\omega)\rvert$	2.73	2.68	2.64	2.59	2.52
$G_m(j\omega)$	-12.75	-16.80	-20.72	-24.65	-28.33
ω_i [rad/s]	0.8	0.9	1.0	1.1	1.2
$\lvert G_m(j\omega)\rvert$	2.46	2.39	2.33	2.26	2.20
$G_m(j\omega)$	-31.83	-35.31	-38.60	-41.70	-44.56

With this data, you can obtain the transfer function of the motor using the commands built into MATLAB. It is the bode plot of the transfer function $G_m(s)$ and $G_m(s)$ of the DC motor obtained through MATLAB.

$$G_m(s) = \frac{1516}{s^2 + 64.18s + 547.7}[\mathrm{V/V}]$$

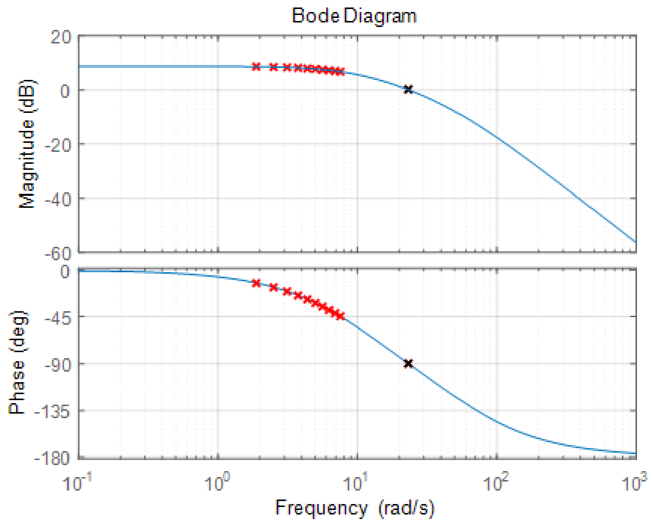

Figure 12. Bode Plot of Motor Transfer Function $G_m(s)$

The following is a rearrange of the transfer function in the form of a standard model of the second-order system we have learned.

$$G_m(s) = \frac{K_m \omega_m^2}{S^2 + 2\zeta\omega_m S + \omega_m^2} = \frac{1516}{s^2 + 64.18s + 547.7}[\mathrm{V/V}]$$

As a result, it can be seen that

$$\zeta_m(damping\ ratio) = 1.37[-]$$
$$\omega_m(natural\ frequency) = 23.40[rad/s]$$
$$K_m(gain) = 2.77$$

3.4. Model validation

To verify the modeling, we need to verify the transfer function of the pulse wave with a lot of frequency components as input because the model should operate at all frequency components. We can see the operation of the motor in the time domain by using the Simulink of MATLAB. We will simulate the input of 0.1$[\mathrm{Hz}]$ output from the oscilloscope to the input of the Simulink and the result of the motor operation obtained through the experiment.

The model is not perfect because there are limited test points in the model and there are errors in the probes. Therefore, verification was done 10 times and the concept of the mean was used.

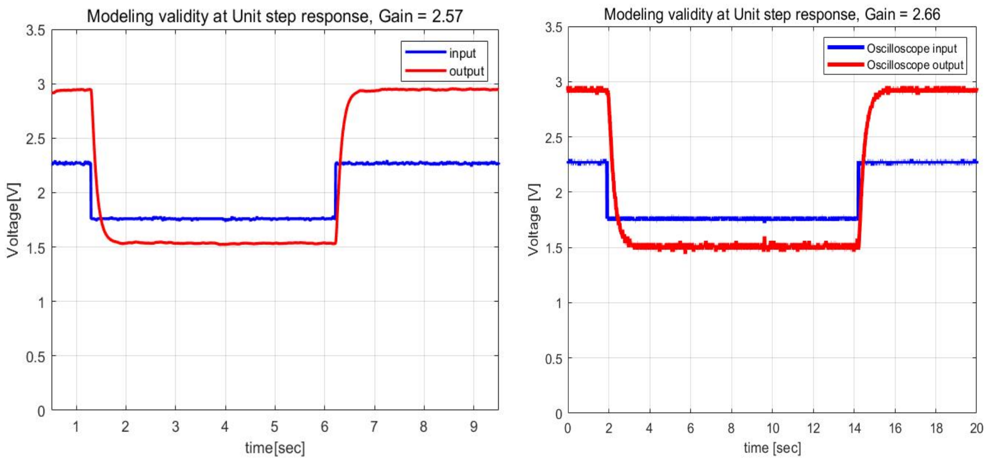

(a) Simulation **(b) Experiment**

Figure 13. Model Validation

The gain is 2.57 in the simulation and 2.66 in the actual motor operation. So check validity as follows, and this modeling is valid.

$$Validity\ Check = \frac{2.66 - 2.77}{2.77} \times 100 = -3.97\%$$

Since the error range is within 5%, this modeling is valid.

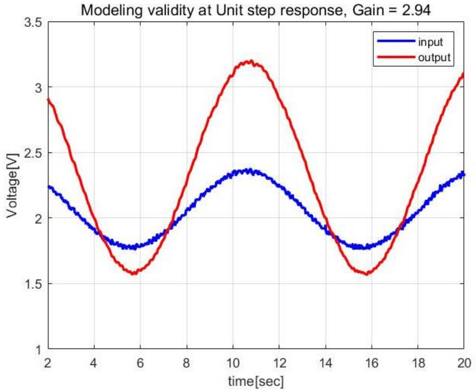

(a) Simulation

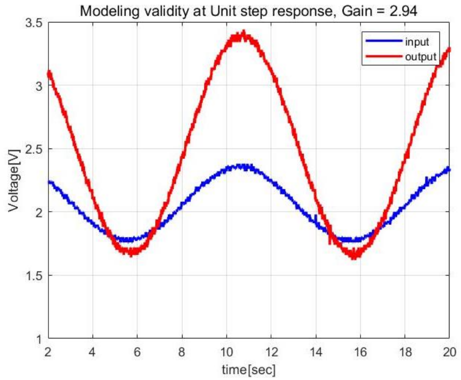

(b) Experiment

Figure 14. Model Validation with sin wave

In sin wave, with same frequency , the gain is 2.94 in the simulation and 2.94 in the actual motor operation. So check validity as follows, and this modeling is valid.

$$Validity\ Check = \frac{2.94 - 2.94}{2.94} \times 100 = 0\%$$

Since the error range is within 5%, this modeling is valid

4. Design Method

4.1. Control gain selection procedure

1) Controller structure selection process

Letting

$$G_c(s) \doteq \frac{N_c(s)}{D_c(s)},\quad G_m(s) \doteq \frac{N_m(s)}{D_m(s)} = \frac{K_m w_m^2}{s^2 + 2\zeta_m w_m s + w_m^2}$$

Results in close-loop system

$$G_{cl}(s) = \frac{N_c(s)N_m(s)}{D_c(s)D_m(s) + N_c(s)N_m(s)}$$

Characteristic equation

$$\Delta G_{cl}(s) = D_c(s)D_m(s) + N_c(s)N_m(s) = 0$$

Table 4. Controller structure

	$G_c(s)$	$\Delta G_{cl}(s)$
P	K_P	$s^2 + 2\zeta_m\omega_m s + (1 + K_P K_m)w_m^2$
PI	$\frac{sK_P + K_I}{s}$	$s^3 + 2\zeta_m\omega_m s^2 + (1 + K_P K_m)w_m^2 s + K_I K_m w_m^2$
PD	$sK_D + K_P$	$s^2 + (2\zeta_m\omega_m + K_P K_m W_m^2)s + (1 + K_P K_m)w_m^2$
PID	$\frac{s^2K_D + sK_P + K_I}{s}$	$s^3 + (2\zeta_m\omega_m + K_D K_m w_m^2)s^2 + (1 + K_P K_m)w_m^2 s + K_I K_m w_m^2$

For pole placement technique, we should be able to move the poles of closed loop system using control gains. In other words, control gains should be included in every term of denominator of closed loop system. Therefore, proper controller structure is ‘PD’ or ‘PID’.

Now we see steady-state error for disturbance

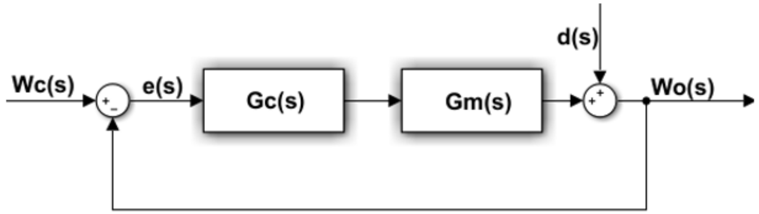

Figure 15. Disturbance block diagram

$$e(s) = \frac{1}{1+G_c(s)G_m(s)} w_c(s) + \frac{-1}{1+G_c(s)G_m(s)} d(s)$$

$|1+G_c(s)G_m(s)|$ becomes larger, $e(s)$ becomes smaller.

Looking at the error for disturbance

Table 5. Error for disturbance

$G_c(s)$	$\left\lvert\frac{e(s)}{d(s)}\right\rvert$	$s=0$ $(w=0)$	$s=\infty$ $(w=\infty)$
PD	$\frac{s^2+2\zeta_m\omega_m s+\omega_m^2}{s^2+(2\zeta_m\omega_m+K_PK_m\omega_m^2)s+(1+K_PK_m)\omega_m^2}$	$\frac{1}{1+K_PK_m}$	1
PID	$\frac{s^3+2\zeta_m\omega_m s^2+\omega_m^2 s}{s^3+(2\zeta_m\omega_m+K_DK_m\omega_m^2)s^2+(1+K_PK_m)\omega_m^2 s+K_IK_m\omega_m^2}$	$\mathbf{0}$	1

At low frequencies, the disturbance rejection is almost perfect.

In addition, type of dc motor is type 0. When the input is step, the steady-state error is zero, and when the disturbance is the triangular reference, the steady-state error is infinite.

Therefore, only PID controllers with pure integrators are possible for disturbance rejection.

In this case, when the input is step, the steady-state error is zero and when the disturbance is the triangular reference, the steady-state error is a constant.

Finally, PID controllers is also necessary because the P controller reflects the current error, the I controller reflects past cumulative errors, and the D controller needs to catch future errors.

Therefore, the controller transfer function

$$G_c(s) = \frac{s^2K_D + sK_P + K_I}{s}$$

The close-loop transfer function

$$G_{cl}(s) = \frac{G_c(s)G_m(s)}{1+G_c(s)G_m(s)}$$
$$= \frac{K_m\omega_m^2(s^2K_D+sK_P+K_I)}{s^3+(2\zeta_m\omega_m+K_DK_m\omega_m^2)s^2+(1+K_PK_m)\omega_m^2 s+K_IK_m\omega_m^2}$$

The denominator of the close-loop transfer function can be expressed as the product of the primary system and the secondary system. Since the control gains are on the close- loop system poles, you can position the poles according to the given specification.

$$\Delta G_{cl}(s) = (s+R_c)(s^2+2\zeta_c\omega_c s+\omega_c^2)$$
$$= s^3+(2\zeta_c\omega_c+R_c)s^2+(\omega_c^2+2\zeta_c\omega_cR_c)s+R_c\omega_c^2$$

The control gain can be expressed by parameter values by the simultaneous equations.

$$\therefore \boldsymbol{K_p} = \frac{\omega_c^2-\omega_m^2+2\zeta_c\omega_cR_c}{K_m\omega_m^2}, \quad \boldsymbol{K_I} = \frac{R_c\omega_c^2}{K_m\omega_m^2}, \quad \boldsymbol{K_D} = \frac{2\zeta_c\omega_c-2\zeta_m\omega_m+R_c}{K_m\omega_m^2}$$

2) Controller gain specification

Based on given specification

① $\%OS < 10\%$

$$\%OS = e^{-\left(\frac{\zeta}{\sqrt{1-\zeta^2}}\right)\pi} \times 100 < 10\%$$

$$\therefore \zeta_c > \sqrt{\frac{(ln10)^2}{(ln10)^2 + \pi^2}} = 0.5912$$

② $t_r^{90} < 0.7$

$$t_r^{90} \cong \frac{2.6535}{w_c} < 0.7 \ @\ \zeta = \frac{1}{\sqrt{2}}$$

$$\therefore \omega_c > 3.7907$$

③ $\zeta_c < 0.90$

Considering t_p, t_s, I set the range so that the system does not get too slow.

④ $\omega_c < 23.40$

$\omega_c \geq \omega_m$ is an unknown world faster than the motor can deliver.

So, it was limited to $\omega_c < \omega_m = 23.40$.

Consider the close-loop pole and zero of the motor and the area of the close-loop pole and zero after add the controller specification.

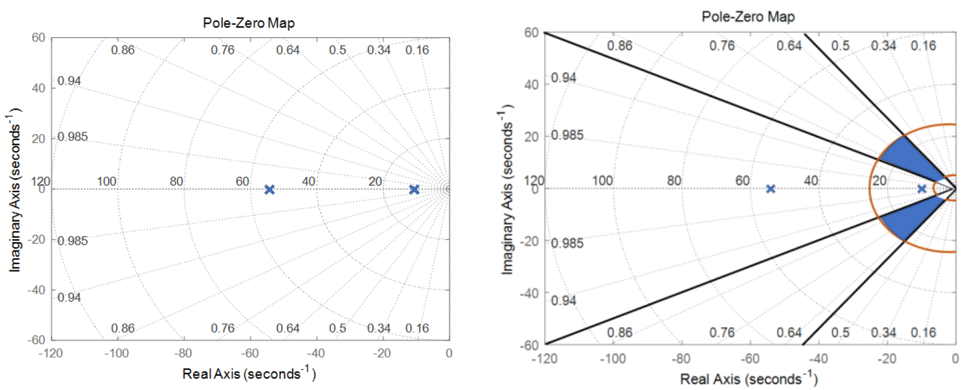

(a) Motor pole-zero map **(b) Controller pole-zero area**

Figure 16. Pole-zero map

3) Controller gain value selection process

① Condition of K_P, K_I, K_D

K_P, K_I and K_D must all be positive.

In the close-loop system, the poles of the first order must be sent away to think of the denominator in a third-to-second approximation. When you think you're sending it five or more times away, assuming that ζ_c is the most ideal 0.707,

$$R_c > 5\,\zeta_c\omega_c = \alpha\omega_c$$

Therefore, α should be at least 3.5.

$$\varpi = \frac{\omega_c}{\omega_m}$$

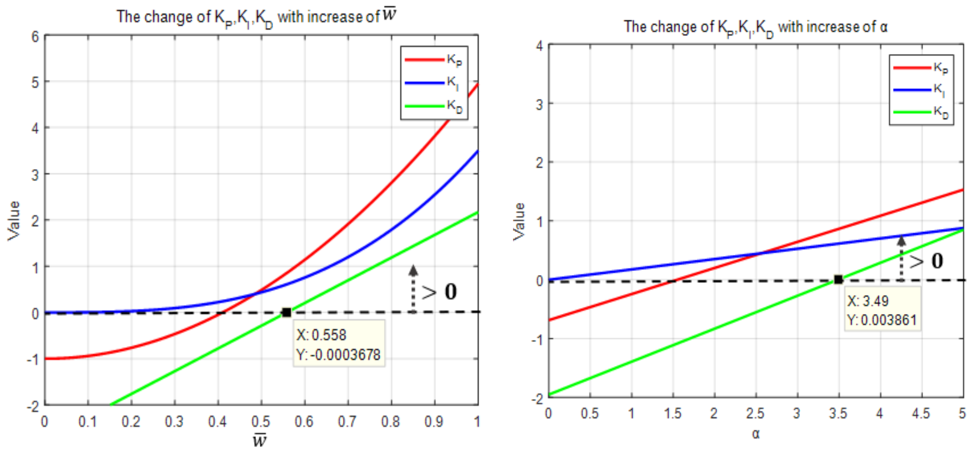

(a) with increase of ϖ **(b) with increase of α**

Figure 17. The change of K_P, K_I, K_D

When $\alpha = 3.5$, minimum value of ϖ satisfying K_P, K_I and $K_D > 0$ is 0.558.

$$\therefore \varpi > 0.558$$

When ϖ = 0.56, the minimum value of α satisfying K_P, K_I and $K_D > 0$ is 3.49.

$$\therefore \alpha > 3.49$$

Since the value of K_D is small and the role of K_D is not visible when ϖ value is minimum, we set a slightly larger value within the range of satisfaction.

Therefore, α was set at 3.5 and ϖ was set at 0.6.

② Condition of $t_r^{90}, \%OS, PM, GM$

The value of α was fixed at 3.5 and considered in terms of time response and frequency response.

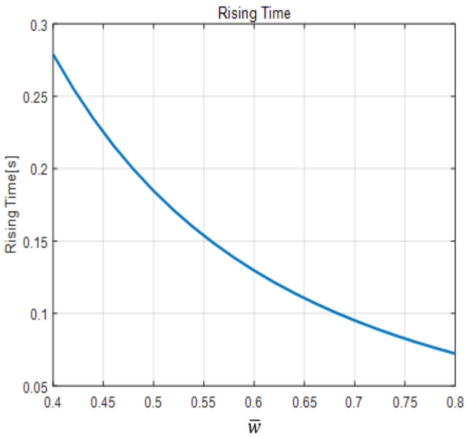

(a) t_r^{90}

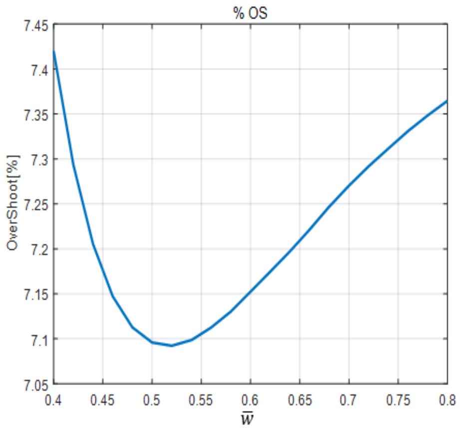

(b) $\%OS$

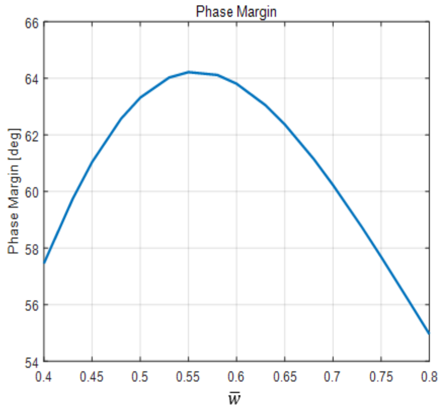

(c) PM

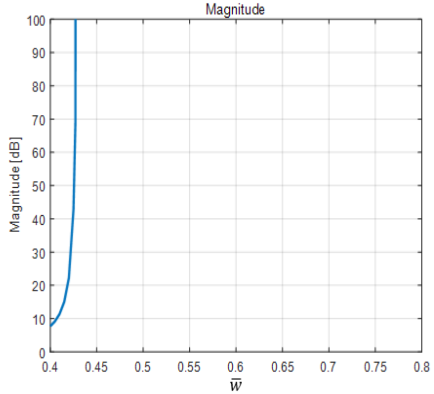

(d) GM

Figure 18. The change of ϖ

From the viewpoint of time response and frequency response, we can confirm that all conditions are satisfied when ϖ is 0.6.

Since the values of α and ϖ are fixed, the values of K_P, K_I and K_D are also determined.

$$K_P = 0.4125, \qquad K_I = 6.3917, \qquad K_D = 0.0032$$

$$G_{cl}(s) = \frac{4.822s^2 + 625.4s + 9690}{s^3 + 69s^2 + 1173s + 9690}$$

The pole and zero of the closed loop system after controller design are as follows.

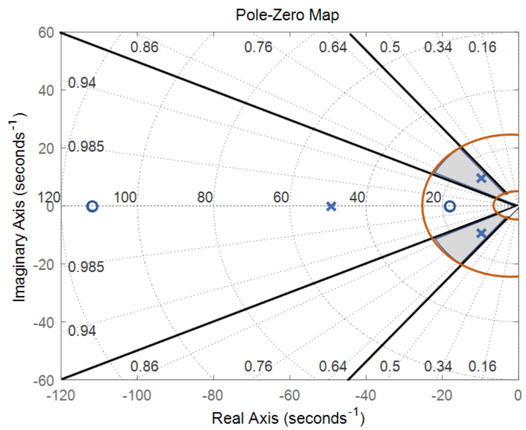

Figure 19. Pole-zero map after controller design

4.2. Initial performance prediction using MATLAB and/or SIMULINK

1) Time response

Let's check the time response from the designed PID. Time response graph shows rise time (t_r^{90}), Over shoot(%OS). The input has a DC offset of 2 [V] and a magnitude of 0.3 [V] pulse wave at a frequency of 0.5[Hz].

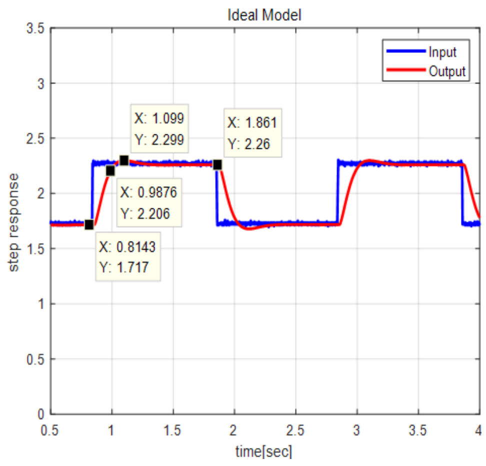

Spec	Standard	Simulation	Validity
t_r^{90}	0.7[sec] >	0.173[sec]	O
%OS	10 % >	7.18 %	O
e_{ss}	0 %	0 %	O

(a) Data plot **(b) Spec Check**

Figure 20. Time response in MATLAB

① Rise time (t_r^{90})

Rising time is the time required for the step response to rise to 90% of the final value and represents the speed of system response time. In the time response, the final value is 2.26[V] and the starting value is 1.717[V]. T_r^{90} is calculated as follows.

$$90\%\ point = (2.26 - 1.717) \times 0.9 + 1.717 = 2.206[\mathrm{V}]$$

$$\therefore t_r^{90} = 0.9876 - 0.8143 = 0.1733[\mathrm{s}]$$

② Over shoot(%OS)

Maximum Overshoot means the most insecure position when input is applied. The overshoot is as follows.

$$\%OS = \frac{y_{max} - y_{ss}}{y_{max} - y_{min}} \times 100 = \frac{2.299 - 2.26}{2.26 - 1.717} \times 100 = 7.18\%$$

③ Additional zero

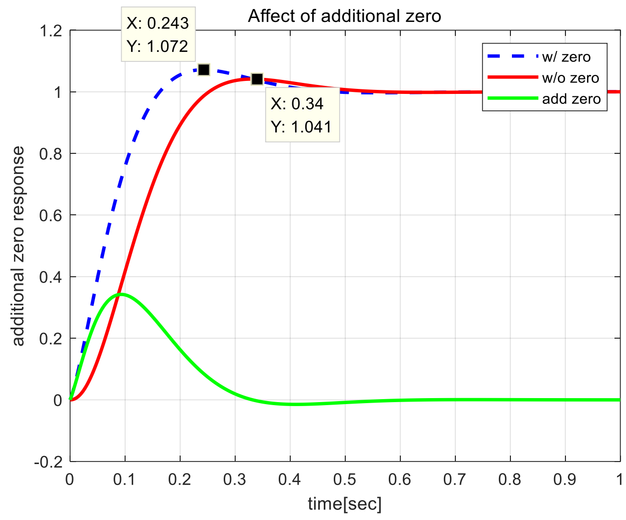

Figure 21. Effect of additional zero

$$G_{cl}(s) = \frac{4.822s^2 + 625.4s + 9690}{s^3 + 69s^2 + 1173s + 9690} = \frac{4.822(s + 17.9884)(s + 111.7200)}{s^3 + 69s^2 + 1173s + 9690}$$

To summarize the equation to see the effect of the dominant pole.

$$\begin{aligned} G_{cl}(s) &= \frac{4.822(s + 17.9884)(s + 111.7200)}{s^3 + 69s^2 + 1173s + 9690} \\ &= \frac{17.9884 * 4.822(\frac{s}{17.9884} + 1)(s + 111.7200)}{s^3 + 69s^2 + 1173s + 9690} \\ &= \frac{17.9884 * 4.822(s + 111.7200)}{s^3 + 69s^2 + 1173s + 9690} + \frac{4.822s(s + 111.7200)}{s^3 + 69s^2 + 1173s + 9690} \\ &= additional\ zero + w/o\ zero \end{aligned}$$

When ignoring the influence of dominant zero, overshoot of 4% corresponds to $\zeta = 0.707$. It can be confirmed that the $\%OS$ is increased and $t_r^{90}$is reduced because of the additional zero.

2) Stability margin

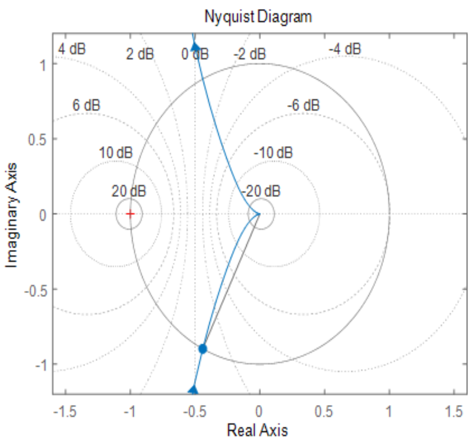

Spec	Margin	Validity	Crossover Frequency
Gain [dB]	Inf	O	Inf [Hz]
Phase [deg]	63.81	O	2.17 [Hz]

(a) Nyquist Plot **(b) Margin Check**

Figure 22. Nyquist data of $G_o = G_c * G_m$

3) Steady state error

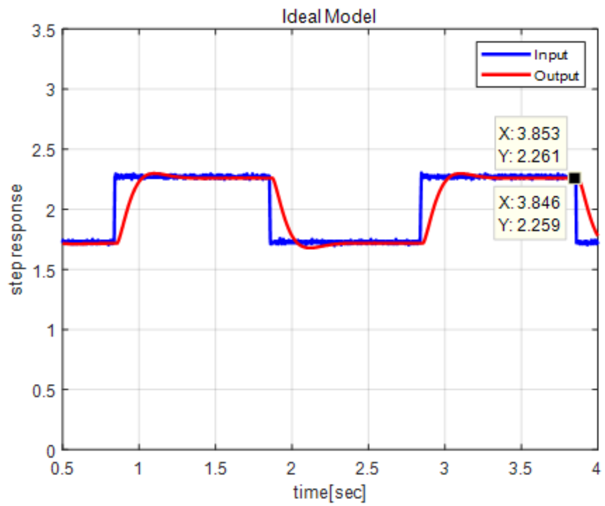

Figure 23. Steady state error data plot

$$e_{ss} = \frac{2.261[\mathrm{V}] - 2.259[\mathrm{V}]}{0.6[\mathrm{V}]} \times 100 = 0.33\%$$

4.3. Implementation of an analog controller using op-amp

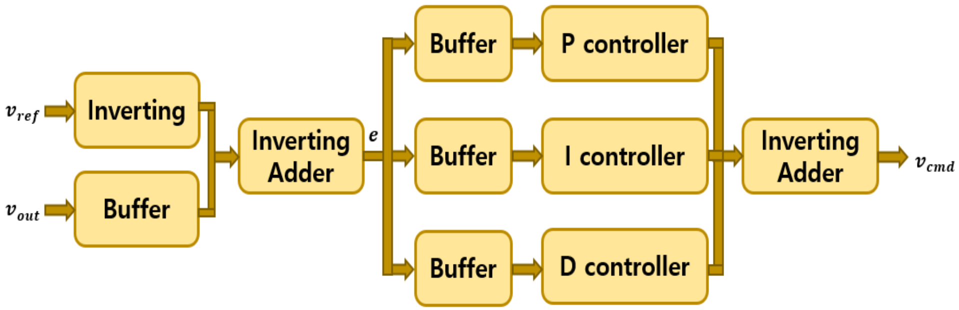

Figure 24. Controller circuit diagram

PID controller will be implemented using op-amp applications. We use buffer because of impedance matching between two different sub-circuits.

1) P controller

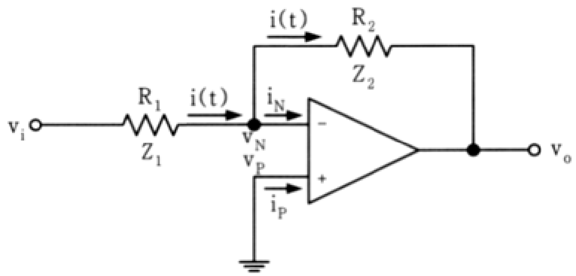

Figure 25. P controller

· **Theoretical value**

$$A_v = \frac{v_o}{v_i} = -\frac{Z_2}{Z_1} = -\frac{R_2}{R_1} = -K_P = -0.4125$$

· **Experiment value**

If the smallest integer ratio of (R_1, R_2) that satisfies $K_P = 0.4125$ is found

$$R_1 = 33[k\Omega], R_2 = 4[k\Omega] \rightarrow K_P = \frac{R_2}{R_1} = 0.4125$$

2) I controller

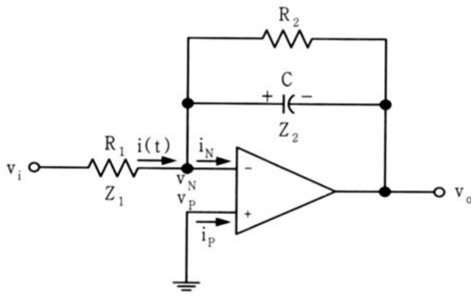

(a) Circuit diagram

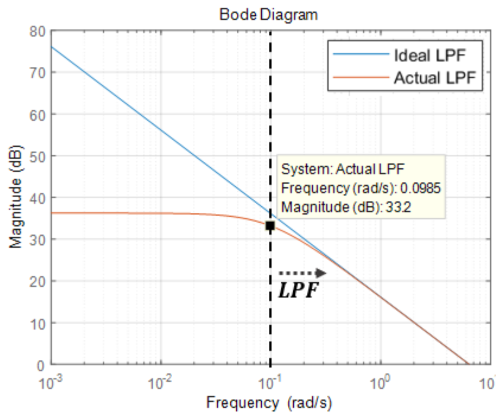

(b) Magnitude of bode plot

Figure 26. I controller

· Theoretical value

$$G(s) = \frac{v_o(s)}{v_i(s)} = -\frac{Z_2}{Z_1} = -\frac{\frac{R_2}{R_2Cs+1}}{R_1} = -\left(\frac{1}{R_1Cs + \frac{R_1}{R_2}}\right)$$

When $\omega_{in} \gg BW_{LPF}$ and $R_2 \gg R_1$, that is, $R_2 > 100R_1$, the ideal integrator type

$$G(s) = -\left(\frac{1}{R_1Cs}\right) = -\left(\frac{K_I}{s}\right) = -\left(\frac{6.3917}{s}\right)$$

From the above results, we can see that the given circuit becomes a low-pass filter. it plays as a integrator in high-frequency

When the frequency used in the motor is more than 0.2[Hz], BW_{LPF} needs to be much smaller than that.

$$0.2 \times 2\pi = 1.26[rad/s] \gg BW_{LPF}$$

· Experiment value

When $C = 101.5[\mu\text{F}]$,

$$R_1 = \frac{1}{K_IC} = \frac{1}{6.3971 \times 101.5[\mu\text{F}]} = 1541[\Omega]$$

It is difficult to satisfy the value of R_1 that satisfies with only one resistor, so $R_1 = 1497[\Omega] + 46[\Omega] = 1543[\Omega]$ is connected in series with a resistor.

Using $R_2 = 100[k\Omega]$, find $BW_{LPF}, G(s)$.

$$BW_{LPF} = \frac{1}{R_2C} = \frac{1}{100[k\Omega] \times 101.5[\mu\text{F}]} = 0.0985[rad/s]$$

$$G_I(s) = -\left(\frac{1}{R_1Cs + \frac{R_1}{R_2}}\right) = -\left(\frac{1}{0.1566s + 0.01543}\right) = -\left(\frac{6.3857}{s + 0.0985}\right)$$

3) D controller

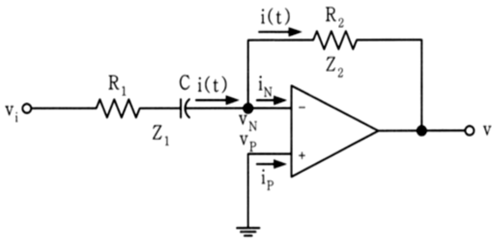

(a) Circuit diagram

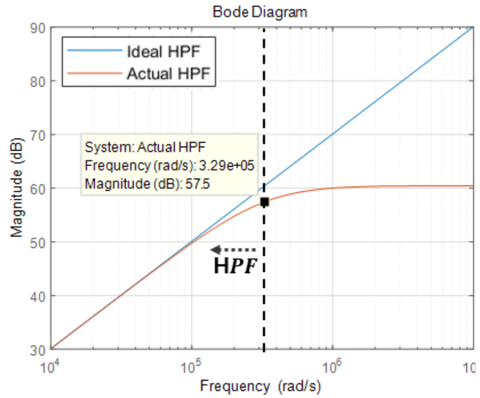

(b) Magnitude of bode plot

Figure 27. D controller

· **Theoretical value**

$$G(s)=\frac{v_o(s)}{v_i(s)}=-\frac{Z_2}{Z_1}=-\frac{R_2}{R_1+\frac{1}{sC}}=-\frac{1}{\frac{1}{R_2Cs}+\frac{R_1}{R_2}}$$

When $\omega_{in} \ll BW_{HPF}$ and $R_2 \gg R_1$, that is, $R_2 > 100R_1$, the ideal differential type

$$G(s)=-(R_2Cs)=-(K_Ds)=-(0.0032s)$$

From the above results, we can see that the given circuit becomes high-pass filter; it plays as a differentiator in low-frequency range

When the frequency used in the motor is small than 4[Hz], BW_{LPF} needs to be much smaller than that.

$$4\times 2\pi = 25.13[rad/s] \ll BW_{HPF}$$

· **Experiment value**

When $C = 101.2[nF]$,

$$R_2=\frac{K_D}{C}=\frac{0.0032}{101.2[nF]}=31.62[k\Omega]$$

It is difficult to satisfy the value of R_1 that satisfies with only one resistor, so $R_2 = 26.98[k\Omega]+4.68[k\Omega]=31.66[k\Omega]$ is connected in series with a resistor.

Using $R_2 = 30[\Omega]$, find $BW_{HPF}, G(s)$.

$$BW_{HPF}=\frac{1}{R_1C}=\frac{1}{30[\Omega]\times 101.2[nF]}=3293800[rad/s]$$

$$G_D(s)=-\left(\frac{1}{\frac{1}{R_2Cs}+\frac{R_1}{R_2}}\right)=-\left(\frac{1055.33s}{s+329380.76}\right)$$

4) PID controller

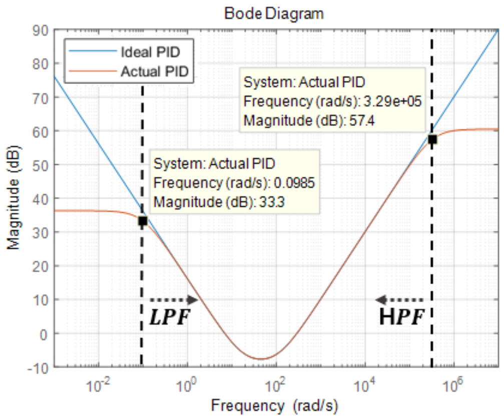

(a) Magnitude of bode plot

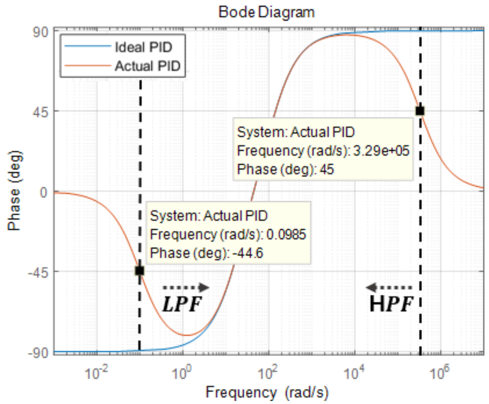

(b) Phase of bode plot

Figure 28. PID controller

Figure shows designed PID controller is coincided with ideal one within frequency range between each bandwidth of LPF and HPF. Since closed loop system poles are in that frequency range, designed PID controller can be regarded as ideal one.

4.4. Overall circuit diagram

The following figure shows the DC motor control circuit connected to the breadboard. The input to the Buffer and Adder on the right is entered and the closed loop system is turned counterclockwise.

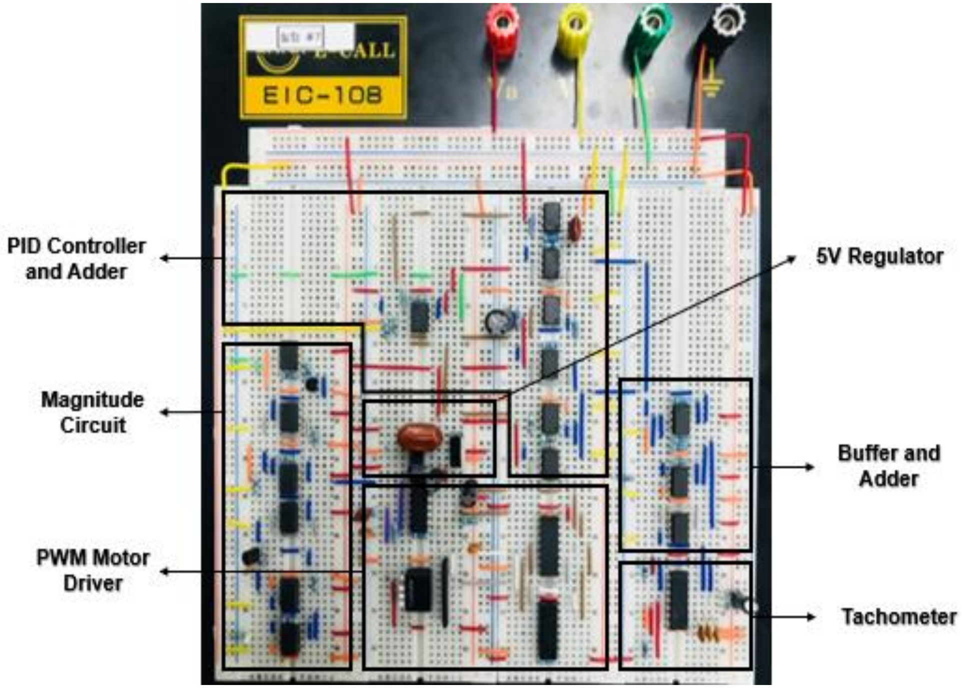

Figure 29. DC motor control circuit on Breadboard

The above circuit can be expressed as a block diagram as follows.

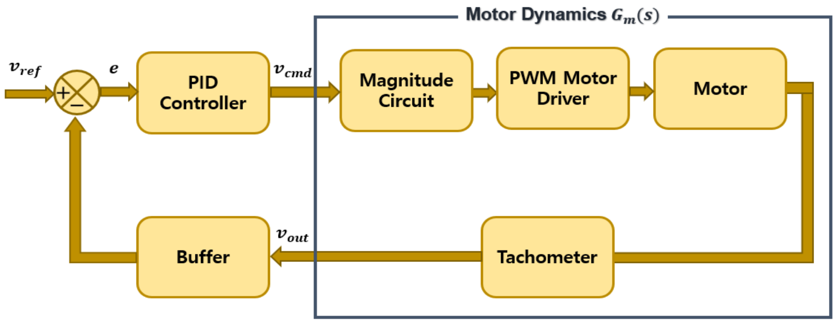

Figure 30. Block Diagram of DC motor control circuit

5. Experimental Result and Analysis

5.1. Precise performance analysis using MATLAB and/or SIMULINK

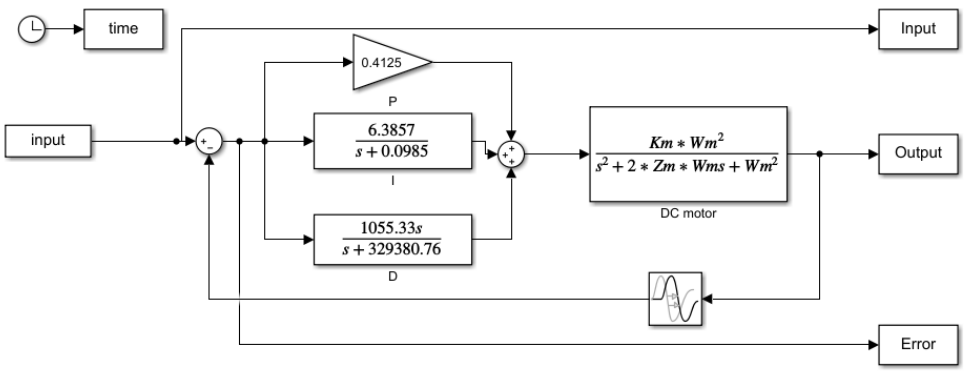

(a) Practical simulation modeling

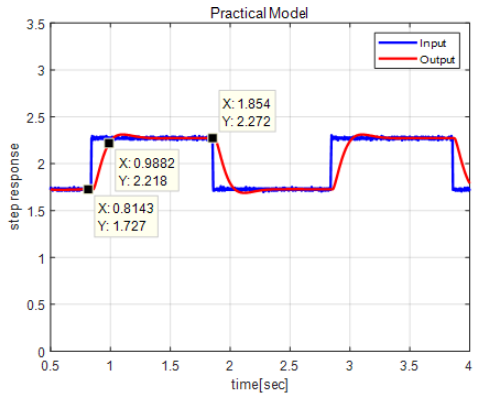

(b) $t_r^{90}[\mathrm{s}]$

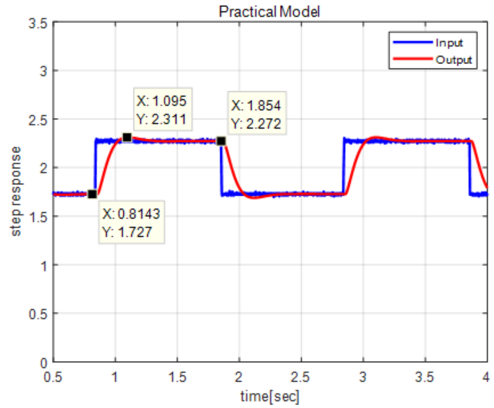

(c) $t_p[\mathrm{s}]$

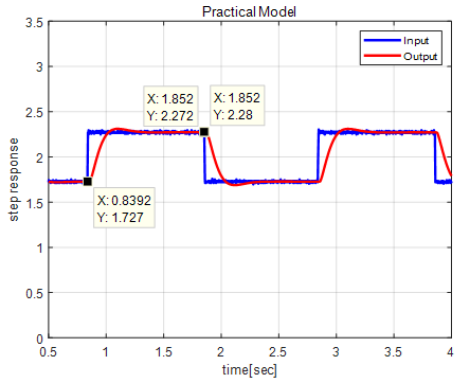

(d) $e_{ss}[\%]$

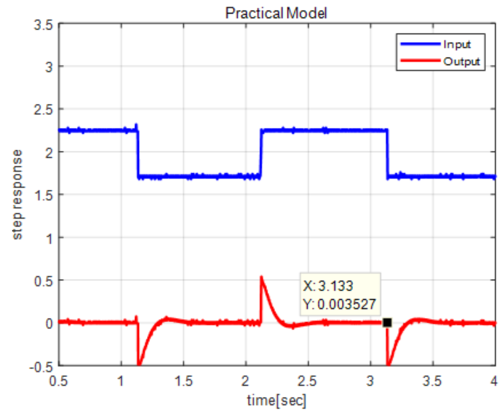

(d) error

	Results
$t_r^{90}[\mathrm{s}]$	0.1739
$overShoot[\%]$	7.16
$e_{ss}[\%]$	1.47[%]
$error$	0.003

(e) Results

Figure 31. Simulink Results

① Simulation Results

$$t_r^{90}[s] = 0.9882[s] - 0.8143[s] = 0.1739[s]$$

$$OS[\%] = \frac{2.311[\mathrm{V}] - 2.272[\mathrm{V}]}{2.272[\mathrm{V}] - 1.727[\mathrm{V}]} \times 100 = 7.16[\%]$$

$$e_{ss}[\%] = \frac{2.280[\mathrm{V}] - 2.272[\mathrm{V}]}{2.272[\mathrm{V}] - 1.727[\mathrm{V}]} \times 100 = 1.47[\%]$$

② Experiment Results

$$t_r^{90}[s] = 1.014[s] - 0.838[s] = 0.176[s]$$

$$OS[\%] = \frac{2.306[\mathrm{V}] - 2.258[\mathrm{V}]}{2.258[\mathrm{V}] - 1.722[\mathrm{V}]} \times 100 = 8.95[\%]$$

$$e_{ss}[\%] = \frac{2.272[\mathrm{V}] - 2.258[\mathrm{V}]}{2.258[\mathrm{V}] - 1.722[\mathrm{V}]} \times 100 = 2.61[\%]$$

5.2. Experimental results

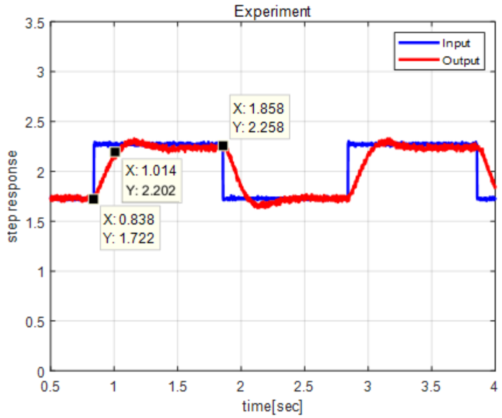

(b) $t_r^{90}[\mathrm{s}]$

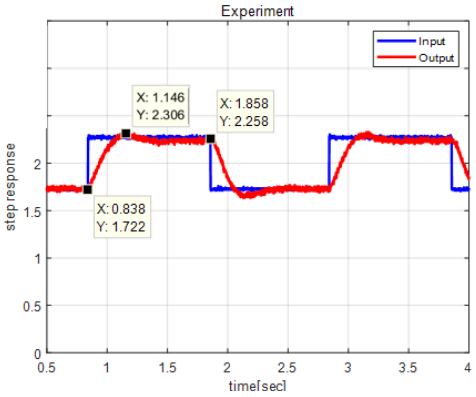

(c) $t_p[\mathrm{s}]$

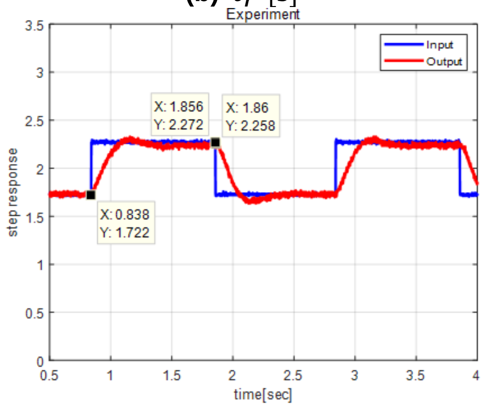

(d) $e_{ss}[\%]$

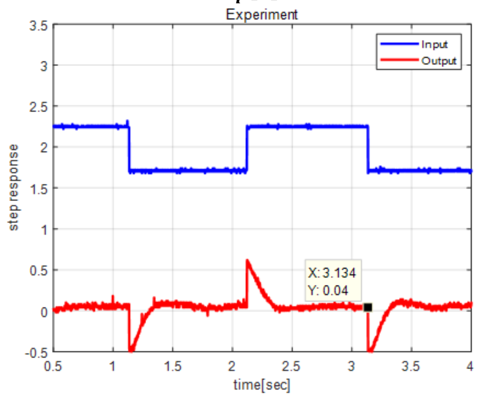

(d) error

	Practical Results	Experiment Results	Validity
$t_r^{90}[s]$	0.1739	0.176	O
$overShoot[\%]$	7.16	8.95	O
$e_{ss}[\%]$	1.47	2.61	X
$error$	0.003	0.04	X

(e) Results

Figure 32. Experiment Results

6. Discussion and Concluding Remarks

① Stability

1) Absolute stability

Determined by yes and no, whether by checking whether all poles are located at LHP of s-plane

2) Relative stability

Robustness against modeling uncertainties

7. Appendices

7.1. Principles of PWM motor driving circuit

PWM is used for all kinds of power control and converter circuits. Generally, there are motor control, DC-DC converter, DC-AC inverter and lamp dimmer. Let's look at the block diagram and pin layout.

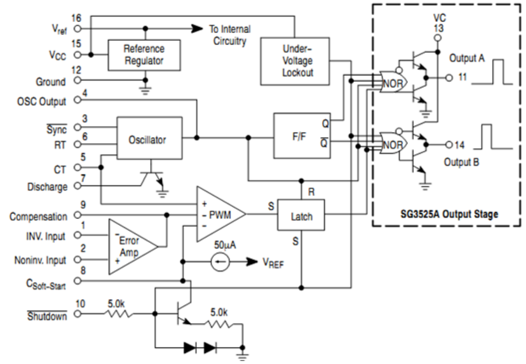

(a) Block Diagram of SG3525

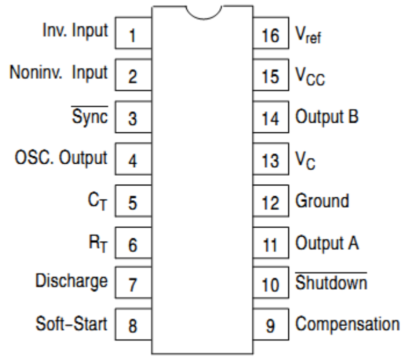

(b) Pin Connections

Pin 1 (inverting input) and 2 (noninverting input) are inputs to the onboard error amplifier. The comparator operates as a comparator that raises or lowers the duty cycle according to the voltage level of the noninverting input (pins 1 and 2). The duty cycle decreases when the voltage on the inverting input (pin 1) is greater than the voltage on the non-inverting input (pin 2), and the duty cycle increases when it is low.

The frequency of the PWM depends on the timing capacitance (CT) connected between pin 5 and ground, and the timing register (RT) connected between pin 6 and ground. The resistance (RD) between pins 5 and 7 determines the dead time and slightly affects the frequency. Therefore, the frequency is related to RT, CT and RD.

$$f = \frac{1}{C_T(0.7R_T + 3R_D)}[\mathrm{Hz}]$$

The value of RD according to the data sheet is 0 Ω to 500 Ω. Therefore, a 100Ω resistor was used and the RT should be in the range of 2kΩ to 150kΩ to 18kΩ, and the CT should be in the range of 1nF to 0.2μF, so it was designed using 0.2μF.

$$f = \frac{1}{0.2\mu(0.7 \times 18\mathrm{k} + 3 \times 100)} = 387.60[\mathrm{Hz}]$$

The other pins are designed with reference to the application circuit of the data sheet. Pin 15 operates with the power supply voltage VCC of the SG3525, pin 12 is the ground connection, and pins 11 and 14 are the outputs from which the drive signal is taken.